BIOCHEMISTRY
including biophysical chemistry & molecular biology

Article

pubs.acs.org/biochemistry

pH Dependence of Amylin Fibrillization

Suman Jha,[†] Jessica M. Snell, Sarah R. Sheftic, Sharadrao M. Patil, Stephen B. Daniels, Frederick W. Kolling, and Andrei T. Alexandrescu*

Department of Molecular and Cell Biology, University of Connecticut, Storrs, Connecticut 06269-3125, United States

Supporting Information

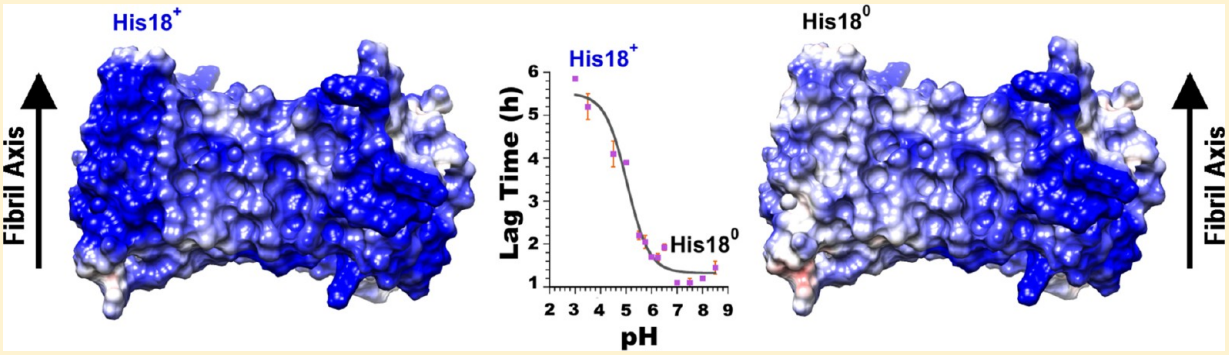

ABSTRACT: In type 2 diabetics, the hormone amylin misfolds into amyloid plaques implicated in the destruction of the pancreatic β-cells that make insulin and amylin. The aggregative misfolding of amylin is pH-dependent, and exposure of the hormone to acidic and basic environments could be physiologically important. Amylin has two ionizable residues between pH 3 and 9: the α-amino group and His18. Our approach to measuring the pK_a values for these sites has been to look at the pH dependence of fibrillization in amylin variants that have only one of the two groups. The α-amino group at the unstructured N-terminus of amylin has a pK_a near 8.0, similar to the value in random coil models. By contrast, His18, which is involved in the intermolecular β-sheet structure of the fibrils, has a pK_a that is lowered to 5.0 in the fibrils compared to the random coil value of 6.5. The lowered pK_a of His18 is due to the hydrophobic environment of the residue, and electrostatic repulsion between positively charged His18 residues on neighboring amylin molecules in the fibril. His18 acts as an electrostatic switch inhibiting fibrillization in its charged state. The presence of a charged side chain at position 18 also affects fibril morphology and lowers amylin cytotoxicity toward a MIN6 mouse model of pancreatic β-cells. In addition to the two expected pK_a values, we detected an apparent pK_a of ~4.0 for the amylin-derived peptide NAc-SNNFGAILSS-NH_2, which has no titratable groups. This pK_a is due to the pH-induced ionization of the dye thioflavin T. By using alternative methods to follow fibrillization such as the dye Nile Red or turbidimetry, we were able to distinguish between the titration of the dye and groups on the peptide. Large differences in reaction kinetics were observed between the different methods at acidic pH, because of charges on the ThT dye, which hinder fibril formation much like the charges on the protein.

Type 2 diabetes accounts for approximately 90% of adult diabetes cases and affects more than 300 million people worldwide.[1] Insulin resistance and high blood glucose levels characterize the disease, but its causes are multifactorial.[2] The endocrine hormone amylin, which normally regulates blood glucose and controls appetite,[3,4] appears to play key roles in the progression of the disease by misfolding into aggregates that are toxic to the pancreatic β-cells that synthesize insulin and amylin.[2−5]

Amylin is a 37-amino acid (3.9 kDa) polypeptide, derived from an 89-amino acid preproprotein.[4] The prosequences are removed by convertases in β-cells; a Cys2−Cys7 disulfide bond is formed, and the C-terminus is amidated to give the mature active form of the hormone. Amylin is intrinsically unstructured in its monomeric state at physiological temperatures and under physiological solution conditions.[6] At high concentrations, amylin misfolds into aggregates with the characteristic intermolecular cross-β-sheet structure of amyloid.[7,8] Consideration of amyloid structures suggests that like charges, replicated along the one-dimensional lattice that constitutes the fibril axis, should energetically disfavor self-association. Thus, electrostatic repulsion could be one of the main forces opposing fibril assembly.[9,10] Compensation of charges displayed on fibril surfaces may also be important in interactions of amyloids with polyanions such as glycosaminoglycans and membrane lipid bilayers.[9,11,12]

Extracellular amyloid deposits of amylin are present in ~90% of patients with type 2 diabetes and are considered a hallmark of the disease. In addition to type 2 diabetes, amylin aggregates also contribute to the failure of human islet cell transplants.[13,14] Genetic evidence linking amylin to type 2 diabetes comes from

Received: August 24, 2013
Revised: December 27, 2013
Published: December 30, 2013

the rare familial S20G mutation, which produces an amylin variant that aggregates more readily[15,16] and is associated with early onset of the disease.[17] The S20G mutation may enhance fibrillization by allowing the β-turn that amylin monomers adopt in the fibril structure to form more readily.[18] In type 2 diabetes, amyloid deposits accumulate in the interstitial fluid between islet cells[3] and cause changes in the morphology of β-cells that have been implicated in their destruction.[3,19] Amylin is toxic when added exogenously to β-cell cultures,[20,21] although as with other amyloid diseases it is unclear whether fibrils or soluble oligomers are responsible for amylin pathology.[22−25] Fibrils could exert their cytotoxic effects by perforating β-cell membranes or by disrupting the network of interactions with other cells in the islets (α, ε, δ, PP) that are necessary for β-cells to function.[4] In another proposed mechanism, it is not the oligomers or fibrils themselves but the process of fibril growth that could be responsible for cytotoxicity, by inducing membrane damage.[26] Finally, it is worth noting that even if fibrils are not the main culprits, their properties are important to understand because fibrils could serve as a reservoir from which toxic oligomers dissociate.[27] In our own studies, we observed that compared to fresh monomeric amylin that can form aggregates *de novo*, mature amylin fibrils formed *in vitro* exhibit weaker albeit significant toxicity when added to a MIN6 mouse insuloma model of pancreatic β-cells.[12] The weaker cytotoxicity of the mature fibrils appears to be concentration-independent, suggesting an equilibrium between nontoxic and toxic species where the population of the latter is determined by a limiting factor, possibly the solubility of the toxic form.[12]

In several transgenic mouse and rat models, overexpression of human amylin has been found to correlate with β-cell apoptosis and diabetes.[28,29] It has been proposed that the aggregation of amylin may start intracellularly, mainly based on evidence from experiments in which human amylin is expressed in transgenic rodents whose own amylin does not form amyloid.[4,28] The initially intracellular origin of fibrils could be due to a defect in the processing of proamylin during the onset of type 2 diabetes.[4,30] Eventually, the amyloid would destroy the β-cell and would be released into the extracellular matrix, where it could serve as a nidus for further amyloid growth.[4] Amylin is present at extremely high concentrations of 0.1−4 mM in the secretory granules of pancreatic β-cells,[31] but there are a number of factors that protect against aggregation. Inside β-cell secretory granules, amylin is stored mainly as the prohormone, which is less prone to aggregation than the processed mature form.[3,30] Interactions between amylin and crystal-like insulin assemblies also protect against fibrillization.[32,33] Finally, the secretory granules have an acidic environment with a pH of 5.5, which inhibits fibril formation.[34] By contrast, the physiological pH of 7.4 for the extracellular matrix, into which amylin is secreted as the mature active hormone, favors fibril formation.[34]

Understanding the pH dependence of amylin fibrillization can shed light on the role of electrostatic charges in amyloid formation, information that in turn could be used to develop drugs that interfere with fibril growth. Amylin is a relatively simple system for studies of the effects of pH on fibrillization, because it has only two ionizable groups near neutrality: the α-amino group at the N-terminus and His18 (Figure 1A). Because the C-terminus is naturally amidated in the mature hormone,[3] it does not titrate with pH. In this work, we examine the pH dependence of amylin fibrillization kinetics to obtain

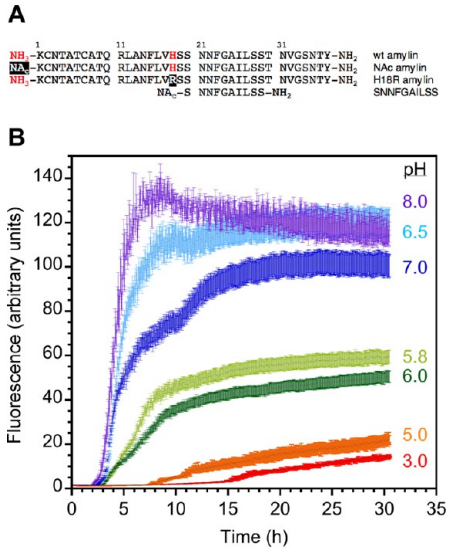

Figure 1. pH dependence of amylin fibrillization. (A) Sequences of wild-type amylin and peptide variants used to characterize the effects of pH on fibrillization. (B) Representative fibrillization reaction curves for NAc-amylin as a function of pH. Uncertainties correspond to the SEM from reactions conducted in triplicate.

apparent ionization constants for the titratable groups in the fibrillar form of the peptide. During the course of our studies, it became apparent that the acid−base chemistry of the dye thioflavin T (ThT), which is commonly used to detect amyloid, also affects the pH dependence of amylin fibrillization. To resolve the contributions, we used the alternate dye Nile Red that does not become ionized over the pH range that was studied.[35] As a second alternative, we followed fibrillization kinetics by turbidimetry.[36,37] We find that residue His18 in the amyloid-forming core of the peptide has a lowered pK_a value, suggesting that protonation of this site is energetically unfavorable for fibrillization. The unfavorable electrostatic interactions resulting from protonation of His18 are weakened with an increasing salt (NaCl) concentration but are still manifested at physiological ionic strength. Protonation of His18 affects fibril morphology as determined by electron microscopy (EM) and cytotoxicity of the peptide to a MIN6[38] mouse model of pancreatic β-cells.

EXPERIMENTAL PROCEDURES

Materials. Human wild-type (wt) amylin, H18R amylin, and the NAc-SNNFGAILSS-NH_2 peptide were custom-synthesized by NeoBioLab (Woburn, MA). NAc-amylin, which has an acetylated N-terminal α-amino group, was custom-synthesized by Biopeptide (San Diego, CA). All peptides were synthesized with an amidated C-terminus, which occurs as a natural post-translational modification in human wt amylin. The wt amylin, H18R amylin, and NAc-amylin peptides contained the naturally occurring Cys2−Cys7 disulfide bond. The peptides were purified to >95% and supplied as dry powders in glass vials of 9 mg each. The samples were taken up in 100% DMSO to form 1.1 mM peptide stock solutions, which were stored in aliquots at −80 °C before being used. For all fibrillization experiments (both fluorescence and turbidimetry), freshly thawed aliquots of the stock solutions were dissolved to a final peptide concentration of 40 μM and a final DMSO concentration of 4% (v/v) in a volume of 200 μL. Ultrapure grade thioflavin T was from

dx.doi.org/10.1021/bi401164k | *Biochemistry* 2014, 53, 300−310

AnaSpec (Fremont, CA), and the dye Nile Red was from Fisher (Pittsburgh, PA). The Alamar Blue dye for measuring cell viability in cytotoxicity assays was from Invitrogen (Carlsbad, CA). All other chemicals used for buffer preparations were from Fisher.

Fibrillization Reactions. A citrate-phosphate buffer was used to maintain the pH of the solutions in the range between 3 and 8.5 used for these studies. To adjust the pH, 10 mM citric acid was titrated against 20 mM dibasic sodium phosphate. For experiments that examined the salt dependence of fibrillization, a 5 M stock solution of NaCl in deionized water was diluted in the different pH buffers to 150 and 300 mM NaCl. Minute differences in solution pH, when they occurred, were adjusted by using 1 M NaOH and HCl solutions. Before amylin was added, all buffers and dye solutions were filtered and degassed for 20 min using a model 500 sonic dismembrator from Fischer Scientific (Waltham, MA) operating at 75% amplitude. Stock solutions of amylin peptides in 100% DMSO stored at −80 °C were thawed and sonicated at 75% amplitude for 5 min to disrupt any preexisting aggregates. To initiate the fibrillization reactions, peptides were added to the pH buffers in the last step, to give a final concentration of 40 μM. The reactions were conducted in white polystyrene 96-well clear bottom plates from Corning (Tewksbury, MA), sealed with a clear polyester sealing tape from Fisher (Agawam, MA). Plates were incubated at 25 °C without agitation. The fluorescence intensity was recorded at 1 min intervals on a Fluoroskan Ascent 2.5 fluorescence plate reader from Thermo Scientific (Rockford, IL). Fibrillization reactions were performed in duplicate or more typically in triplicate, to check reproducibility and obtain uncertainties in the kinetic parameters describing the reactions. In total, more than 900 fibrillization reactions were performed to characterize the pH and NaCl dependence of amylin fibrillization described in this work.

For reactions monitored by ThT, a dye concentration of 20 μM was used. The excitation and emission wavelengths were 440 and 490 nm, respectively. To rule out pH-dependent binding of the ThT dye to fibrils, a control experiment was conducted with fibrils preformed at pH 4 or 8. The fibrils were resuspended in buffers ranging from pH 3 to 8.5, and the ThT fluorescence was measured. The fluorescence was constant across the pH range, ruling out pH-dependent interactions of the ThT dye and preformed fibrils. Similarly, the fluorescence of the free ThT dye did not change significantly with pH. For reactions monitored with Nile Red, a dye concentration of 5 μM was used due to its lower solubility in aqueous solutions. The excitation and emission wavelengths for Nile Red were 544 and 590 nm, respectively (Figure S1 of the Supporting Information). Turbidimetry experiments were conducted by measuring the optical density at 372 nm on a Synergy HT absorbance plate reader from Bio-Tek (Winooski, VT).

Data Analysis. Lag times were measured graphically, as the x-axis value at the intersection of the lag phase slope and the slope of the steepest part of the fibril growth phase.[39] Growth phase rates were obtained by omitting the time points for the lag phase and using a nonlinear least-squares fit of the remainder of the data to the exponential function $y = A + B\exp(-kx)$, where k is the growth rate.[39] ThT fluorescence plateaus were obtained graphically from the maximal steady-state fluorescence intensities of the fibrillization curves, neglecting fluctuations in the data that occur due to light scattering from particulate aggregates as the fibrillization reaction proceeds to completion.[40] Data on the pH dependence of fibrillization parameters such as lag times, elongation rates, and fluorescence plateaus were fit to the Henderson−Hasselbalch equation $\delta = \delta_{acid} - [(\delta_{acid} - \delta_{base})/(1 + 10^{pK_a - pH})]$, where δ_{acid} is the limiting spectral value at acidic pH (e.g., fluorescence or optical density), δ_{base} is the limiting spectral value at basic pH, and pK_a is the negative log of the ionization constant. The δ_{acid}, δ_{base}, and pK_a values were treated as free variables in nonlinear least-squares fits of the data to the Henderson−Hasselbalch equation. We typically did not include a parameter for the cooperativity of ionization (the Hill coefficient), because F tests on the limiting ratio of reduced χ^2 ratios[41] for the three- and four-parameter fits indicated that for most of the data sets inclusion of the extra free variable was not justified. The pK_a values from three- or four-parameter fits were very close, typically within the uncertainties of the least-squares fits.

NMR pH Titrations. NMR experiments were performed on a Varian Inova 600 MHz instrument equipped with a cryogenic probe. Reference pK_a values for the α-amino group and His18 were determined from one-dimensional ^{1}H NMR titrations of a 50 μM monomeric human amylin sample in D_2O at 25 °C. A pK_a of 6.45 ± 0.14 was obtained from the Hε1 proton of His18, which titrates from 7.65 ppm at basic pH to 8.60 ppm at acidic pH. A pK_a of 8.20 ± 0.12 was obtained from the Hα proton of Lys1, which titrates from 3.50 ppm at basic pH to 3.73 ppm at acidic pH. The pK_a values of monomeric amylin were in excellent agreement with those of random coil peptides: 6.5 for a histidine and 8.0 for an α-amino group.[42]

In separate experiments, we used one-dimensional ^{1}H NMR to follow the pH dependence of the dye ThT in 99.96% D_2O. We saw no changes in the spectrum between pH 9.5 and 2.5. Below pH 2.5, a resonance corresponding to the H3′ proton of ThT titrates from 6.9 to 8.1 ppm. Smaller perturbations were also seen for the methyl groups from the dimethylamine nitrogen substituent at position 4′.[43] The resonances titrated with an apparent pK_a of 1.5, corresponding to the protonation of the dimethylamine group.[44] The standard DSS (4,4-dimethyl-4-silapentane-1-sulfonic acid) was used as an internal chemical shift reference for all NMR experiments.

Transmission Electron Microscopy. Samples containing 100 μM amylin at pH 7.4 or 4.0 were incubated at 25 °C, and aliquots of the reaction were removed after 1 week. For the experiments with NAc-amylin and H18R amylin at pH 7.4, the peptide concentrations were 80 μM and the samples were incubated for 2 days at 37 °C to form fibrils. Aliquots from the fibrillization reaction mixtures were blotted for 1−3 min onto carbon-coated 400 mesh Maxtaform copper grids (Ted Pella Inc., Redding, CA), followed by negative staining with 1% uranyl acetate. EM images were recorded on an FEI Tecnai G_2 Spirit BioTwin transmission electron microscope equipped with an AMT XR-40 camera, which is part of the UConn EM facility.

Cytotoxicity Assays. Stock solutions of wt amylin, NAc-amylin, and H18R amylin were prepared to an approximately 8 mM peptide concentration by dissolving lyophilized samples in 100% DMSO. The concentrations of the stock solutions were then measured using the Micro BCA Protein Assay Kit from Thermo Scientific. The stock solutions were diluted using fetal bovine serum (FBS)-free Dulbecco's modified Eagle's medium (DMEM) and sonicated continuously for 5 min at 75% amplitude to disrupt any preexisting aggregates. FBS was added just before use, to a concentration of 15% (v/v). The final

concentrations of peptides for all cytotoxicity experiments were 80 μM, and the final DMSO concentration was 1% (v/v).

Cytotoxicity experiments were conducted using the MIN6 mouse insuloma cell line model of β-pancreatic cells,[38,45] which was a gift from A. Rustgi (University of Pennsylvania, Philadelphia, PA). Cells were seeded to a density of 20000 per 100 μL well, in black clear-bottom 96-well plates from BD Biosciences (San Jose, CA). The cells were grown in DMEM fom Invitrogen (Carlsbad, CA) supplemented with 15% fetal bovine serum, 25 mM glucose, 2 mM L-glutamine, 500 mM sodium pyruvate, 55 μM β-mercaptoethanol, 1000 units/mL penicillin, and 100 μg/mL streptomycin. After incubation for 24 h at 37 °C in a humidified incubator with 5% CO_2, the culture medium was removed and replaced with fresh medium containing wt amylin, NAc-amylin, H18R amylin, or controls. The cells were incubated for an additional 20 h followed by addition of 10% (v/v) Alamar Blue. Fluorescence due to the reduction of the Alamar Blue dye by viable cells was measured after 6 h on a Fluoroskan Ascent 2.5 fluorescence plate reader. The excitation and emission wavelengths were 544 and 590 nm, respectively. The cell viability (percent) was calculated from the ratio of Alamar Blue fluorescence in treated cells to cells seeded in medium alone. Uncertainties were calculated from the standard errors of measurements conducted in triplicate.

RESULTS

pH Dependence of Amylin Fibrillization Kinetics. The α-amino group and His18 (indicated in red type in Figure 1A) are the only two groups in wt amylin that titrate between pH 3 and 9. The other ionizable groups, Lys1, Arg11, and Tyr37, should titrate only at extremes of pH as their random coil pK_a values are 10.4, 12.0, and 9.8, respectively.[42] To distinguish between the contributions of the N-terminus and His18, we used two peptides that retain only one of the titratable groups each. In NAc-amylin, the α-amino group is blocked by acetylation (reverse type in Figure 1A) and His18 is the only titratable group. In H18R amylin, the histidine is replaced with an arginine and the α-amino group is the only site affected by pH. As a control, we also used the short NAc-SNNFGAILSS-NH_2 peptide, corresponding to the "amyloidogenic segment" of amylin comprised of residues 20–29.[4,46] Both the α-amino and α-carboxyl groups are blocked in this peptide so that there are no pH-titratable groups.

To characterize the pH dependence of amylin fibrillogenesis, we conducted fibrillization reactions on wt amylin and the peptide variants shown in Figure 1A, at 13 pH values distributed between pH 3.0 and 8.5. Representative data for these reactions are shown for NAc-amylin in Figure 1B. The fibrillization reactions can be characterized in terms of three parameters that were calculated using methods described in the literature.[39] The lag time is related to the formation of critical nuclei, before any fibrils are detected (Figure 2A). The growth rate describes the addition of monomers to preexisting fibrils (Figure 2B). The ThT fluorescence plateau is the maximal signal as the reaction enters an apparent steady state (Figure 2C). The lag times were generally more precisely determined than the fluorescence plateaus, while the fibril growth rates gave the largest experimental uncertainties.

Fibrillization is enhanced with an increase in pH (Figure 2 and Figure S2 of the Supporting Information). With the change from acidic to basic pH, the lag times for the reaction decrease (Figure 2A), while the growth rates (Figure 2B) and fluorescence plateaus increase (Figure 2C). While the data in

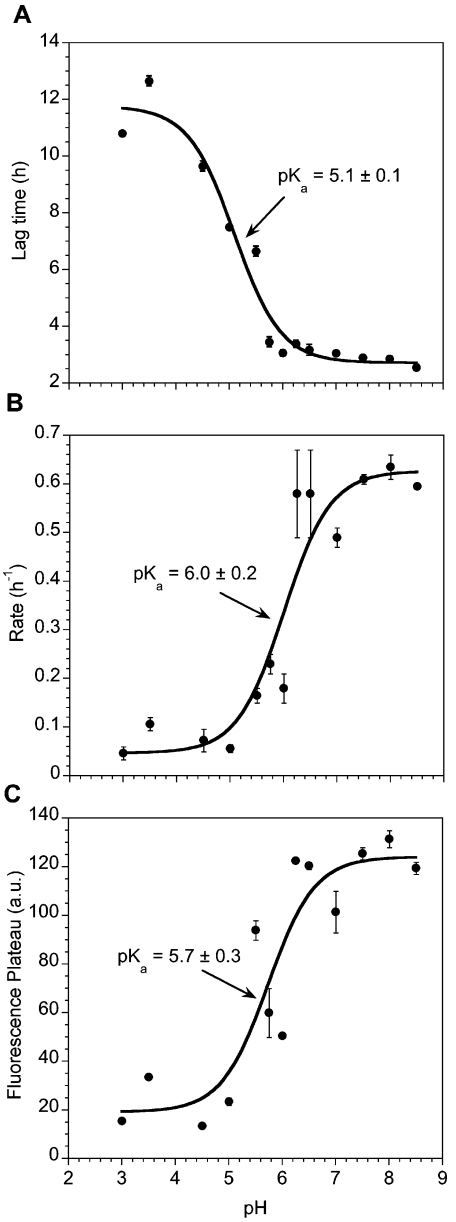

Figure 2. pH dependence of kinetic parameters for the fibrillization of NAc-amylin: (A) lag times, (B) fibril elongation rates, and (C) ThT fluorescence plateaus. The pK_a values obtained from nonlinear least-squares fits of the kinetic data to the Henderson–Hasselbalch equation are given in each panel. Uncertainties for each data point correspond to standard errors from reactions conducted in triplicate, while the uncertainties in the pK_a values are standard errors from the least-squares fits. In this and subsequent figures, errors are shown for all data points but in some cases are smaller than the symbols used to represent the data.

Figure 2 are shown for NAc-amylin, the same trends are seen for wt amylin and H18R amylin (Figures S3 and S4 of the Supporting Information). The increase in ThT plateaus with an increase in pH suggests that more fibrils are formed under basic than acidic conditions (Figure 2C). This is not necessarily the case, because the ThT fluorescence could also be affected by differences in the affinity or binding mode of the dye[47] for fibrils formed with different surface properties at different pH values. In the case of amylin, however, separate electron microscopy (EM) and total internal reflection fluorescence

dx.doi.org/10.1021/bi401164k | Biochemistry 2014, 53, 300–310

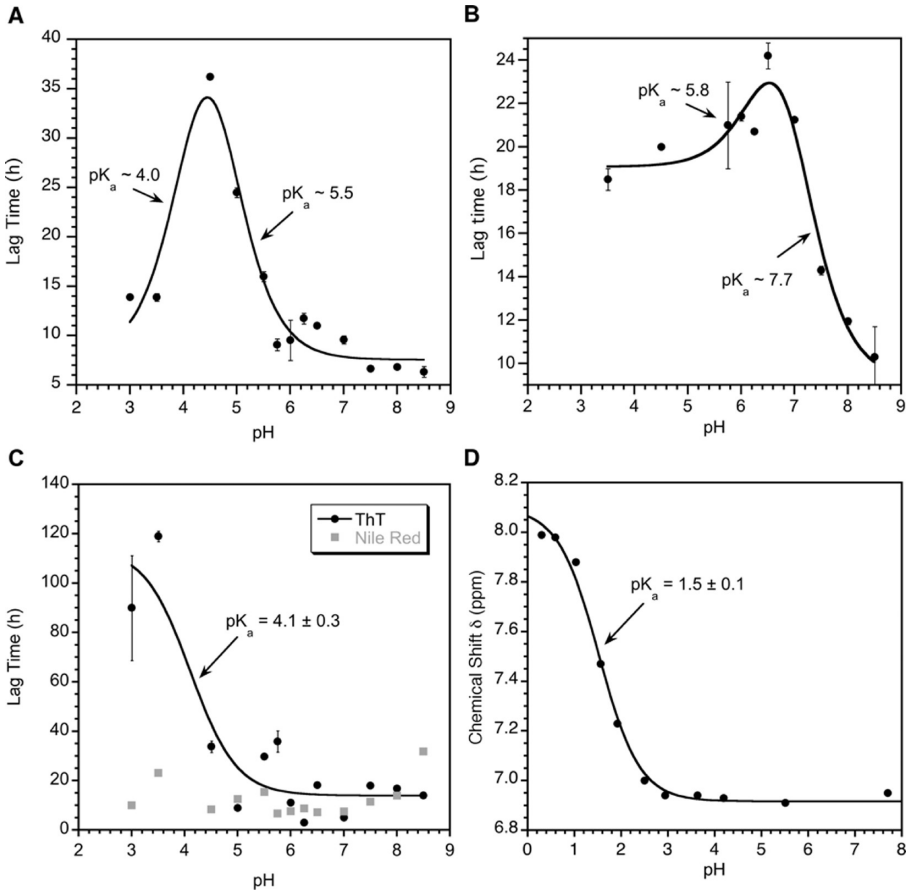

Figure 3. Contributions of ThT to the pH dependence of amylin fibrillization. (A) pH profile of wt amylin lag times monitored by ThT fluorescence. (B) pH profile of H18R amylin lag times detected by ThT fluorescence. (C) pH dependence of lag times for the NAc-SNNFGAILSS-NH_2 peptide characterized by ThT (circles) or Nile Red fluorescence (squares). (D) NMR pH titration of an aqueous solution of the free dye ThT, monitoring the ionization of the dimethylamine group from the H3′ resonance.

microscopy (TIRFM) studies have shown that many more fibrils are formed at basic than at acidic pH.[48] The enhanced fibrillization of amylin at high pH and the trends observed in the pH dependence of the kinetic parameters summarized in Figure 2 are consistent with two previous studies in which wt human amylin was examined at only two pH values, acidic and neutral.[34,49] With the more extensive pH data in this study, we can determine that all three parameters that describe the fibrillization of NAc-amylin titrate with apparent pK_a values of ∼5 or ∼6 (Figure 2), suggestive of acid−base reactions involving a histidine. Although His18 is the only pH-titratable site in NAc-amylin, we will show that the apparent pK_a values determined with the dye ThT contain a composite contribution from the pH titration of groups on the peptide as well as the dye.

Effects of Dyes on Fibrillization Kinetics. In contrast to NAc-amylin, the lag times of human wt amylin in the absence of added salts show a biphasic pH dependence, with two pK_a values of ∼4.0 and ∼5.5 (Figure 3A). The pK_a of 5.5 could be due to His18, but there are no additional groups in the peptide that could explain the second pK_a at 4.0, because the C-terminus of the peptide is amidated. An additional weak shoulder is observed for wt amylin between pH 6 and 9, which could correspond to the titration of the α-amino group (Figure 3A). The biphasic pH profile was probably missed in previous studies that examined wt amylin at only two pH values above pH 4.0.[34,49] A similar biphasic pH dependence is seen for the lag times of H18R amylin (Figure 3B), in which the only pH-titratable site is the α-amino group. The pK_a of 7.7 observed for H18R amylin closely matches the random coil value of 8.0 for an α-amino group.[8,50] Note that the magnitude of the 2-fold changes in lag times between pH 6.5 and 9 for the α-amino group in H18R (Figure 3B) are much smaller than the corresponding 7-fold changes in lag times due to His18 in wt amylin (Figure 3A), consistent with the N-terminus of the peptide being unstructured in the fibrils.[8,50] The second pK_a value of ∼6.0 in H18R (Figure 3B) cannot be ascribed to any groups in the peptide, so we suspected that the lower pK_a values observed for both wt amylin and H18R amylin are due to protonation of the dimethylamino group of ThT,[44] which was used to monitor the fibrillization reactions (Figure 4). The biphasic pH dependence is not observed for NAc-amylin (Figure 3A), perhaps because the pK_a values for the ThT dye (∼4.0) and His18 (∼5.0) are too close to resolve.

To test the hypothesis that the acidic pK_a seen for wt and H18R amylin is due to the dye ThT, we performed pH-dependent fibrillization studies with the short NAc-SNNFGAILSS-NH_2 peptide, which has no intrinsic titratable groups. In the absence of added salt, we observed a pK_a of 4.1 in the pH dependence of the lag times for fibril formation monitored by ThT (black circles in Figure 3C). Roughly the same pH dependence was observed for the rates of fibril elongation and for the ThT fluorescence plateaus of the NAc-SNNFGAILSS-NH_2 peptide in reactions performed without salt (Figure S5 of

dx.doi.org/10.1021/bi401164k | Biochemistry 2014, 53, 300−310

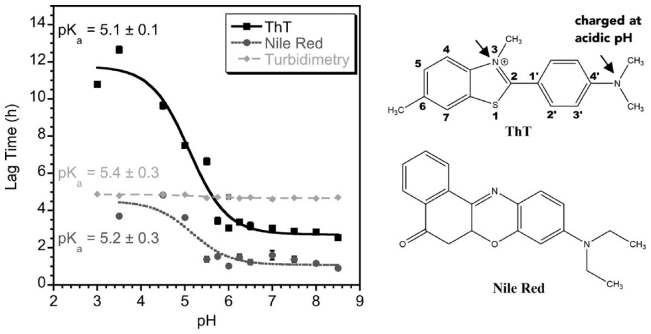

Figure 4. pH dependence of lag times for NAc-amylin fibrillization when fibrils are detected using different methods: (squares) ThT fluorescence, (circles) Nile Red fluorescence, and (diamonds) turbidimetry at 372 nm. The structures of ThT and Nile Red are shown. The numbering scheme for ThT was taken from the literature.[43]

the Supporting Information). The pH dependence is not observed when the fibrillization reactions are detected with the alternate dye Nile Red (gray squares in Figure 3C), which in contrast to the dye ThT is pH-insensitive over the range of pH values we studied.[35,51] Similarly, the biphasic pH profile due to ThT seen for lag times of wt amylin and H18R amylin in the absence of salt (Figure 3A,B) is not seen when the reactions are monitored with the alternate dye Nile Red (Figures S6–S8 of the Supporting Information) or by turbidimetry[36,37] at 372 nm (Figure S9 of the Supporting Information). Taken together, these observations strongly suggest that the pK_a of ∼4.1 observed when fibrillization reactions are monitored with ThT in the absence of salt is due to protonation of the dimethylamine group of the dye.[44]

To gain further insight into the acid–base chemistry of the dye ThT, we monitored the pH titration of the free dye in aqueous solution using NMR. As shown in Figure 3D, the 3′ aromatic ring protons of ThT[43] titrate with a pK_a of 1.5. The pK_a value of the free dye is some 3 pH units lower than that obtained from fibrillization studies with the NAc-SNNFGAILSS-NH_2 peptide (Figure 3C). There are a number of factors that could be responsible for this large pK_a shift. First, in the NMR experiments, we are looking at the ground state of the dye, whereas in the fluorescence experiments, we are looking at the excited state of the dye after it has absorbed a photon. The excited and ground states have different electronic structures and thus could have markedly different pK_a values. Second, in the fluorescence experiments, we are looking at the dye embedded in the hydrophobic environment of amyloid fibrils, which could shift the pK_a compared to the value for the free dye in an aqueous solution. Finally, in solution, the ThT dye has free torsional rotation about the bond connecting the benzothiazole and dimethylaminobenzene rings (Figure 4). Rotation about this bond is restricted when the dye is bound to fibrils, which leads to the characteristic marked increase in fluorescence when ThT is bound to amyloid fibrils.[52] The restricted conformational freedom of ThT when bound to fibrils could also perturb the pK_a of the dye compared to that in solution.

Figure 4 compares the pH dependence of the lag times for NAc-amylin fibril formation monitored by different methods: the dye ThT (squares), the dye Nile Red (circles), and turbidimetry (diamonds). The apparent pK_a values obtained by the different methods are identical within experimental error (Figure 4). In contrast, the kinetic lag times for fibril formation show large increases with ThT below pH 5, when the dye carries two charges as opposed to none for Nile Red. Smaller differences in lag times are seen at basic pH values where ThT carries a single charge while Nile Red is uncharged. The pH profile obtained by turbidimetry is relatively flat compared to those obtained with ThT or Nile Red but gives a pK_a of 5.4 (for an expansion, see the purple curve in Figure S9 of the Supporting Information). The differences in the pH dependence of the lag times when monitored by turbidimetry and the dyes, suggest that the dyes modulate interactions between charges on the fibrils and hence the reaction kinetics, with the effects being particularly large for ThT in its doubly ionized state below pH 5.

Effects of Salt on Interactions of the Dye ThT and Amylin Fibrils. The pH-dependent electrostatic interference between the dye ThT and amylin fibrils appears to be restricted to low-solution ionic strength conditions. When fibrillization reactions with the NAc-SNNFGAILSS-NH_2 peptide were conoducted in the presence of the dye ThT together with 150 or 300 mM NaCl, we observed no pH dependence on the kinetics of fibrillization, in contrast to the reactions conducted in the absence of added salts (Figure S5 of the Supporting Information). In agreement, the biphasic pH dependence observed for wt amylin and H18R amylin was largely suppressed when the reactions with ThT were conducted in the presence of 150 or 300 mM NaCl (Figures S3 and S4 of the Supporting Information), except that a reduced biphasic pH dependence was still seen at 150 mM NaCl for the plateaus of H18R (Figure S4 of the Supporting Information). Finally, the inhibition of NAc-amylin fibrillization observed at acidic pH with ThT compared to that with Nile Red (Figure 4) was relieved in the presence of salt, with the lag times for the reactions monitored by the two dyes becoming more similar at 150 or 300 mM NaCl (Figure S10 of the Supporting Information) than in the absence of salt.

Apparent pK_a Values for His18 and the α-Amino Group of Amylin. Having discriminated between the contributions of groups from the peptide and ThT to the pH dependence of amylin fibrillization, we were able to unambiguously determine pK_a values for the two pH-titratable sites in amylin using Nile Red and turbidimetry. For His18, both Nile Red and turbidimetry give an apparent pK_a of ∼5.0 for NAc-amylin in the absence of salt (Figure 4). This value is lowered by ∼1.5 pH units from the random coil pK_a of 6.5 for a histidine,[42] or the pK_a value of 6.4 measured by NMR for His18 in monomeric amylin that is intrinsically unfolded. The lowered pK_a of His18 in the fibrils indicates that a higher proton concentration (lower pH) is needed to place a positive charge on this site, and that ionization of the histidine disfavors fibril formation. Protonation of the histidine at low pH leads to longer lag times, reduced fibril elongation rates, and reduced steady-state plateaus (Figures 2 and 4 and Figure S6 of the Supporting Information), all of which indicate that fibril formation is inhibited at acidic compared to neutral pH.

Measurements for the N-terminal α-amino group were made difficult by the pK_a of this group being close to the basic limit of the pH range we studied (pH 8.5). Nevertheless, we were able to determine a pK_a value of 7.7 for the α-amino group in the H18R amylin peptide from the ThT data (Figure 3B). Consistently, the Nile Red and turbidimetry data indicate a pK_a between 7 and 8 for the α-amino group in H18R amylin (Figures S8 and S9 of the Supporting Information), in

dx.doi.org/10.1021/bi401164k | *Biochemistry* 2014, 53, 300–310

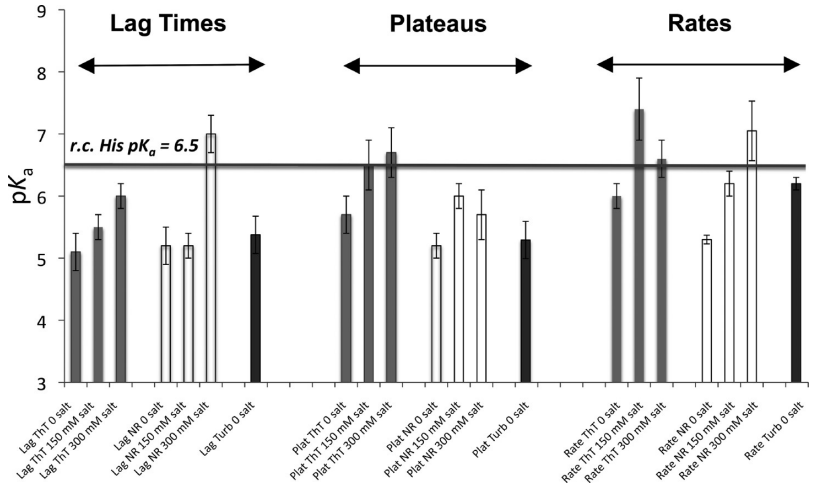

Figure 5. NaCl dependence of pK_a values obtained from different kinetic parameters that characterize the fibrillization of NAc-amylin. Fibril formation was monitored by ThT fluorescence (gray), Nile Red fluorescence (white), or turbidimetry (black). Turbidimetry measurements were taken only in the absence of salt. The horizontal line indicates the random coil pK_a value of a histidine.

agreement with the random coil value of 8.0[42] and the value of 8.2 measured for the α-amino group in unfolded monomeric amylin by NMR. Whereas His18 participates in the intermolecular hydrogen-bonded β-sheet of amylin fibrils,[50] the first eight amino acids at the N-terminus are disordered.[8,50] As with His18, charging of the α-amino group at low pH inhibits fibrillization as manifested by increased lag times (Figure 3b) and decreased fibrillization rates (Figures S8 and S9 of the Supporting Information). This suggests that even though the N-terminus of amylin is disordered in the fibrils, charging of the α-amino group leads to long-range electrostatic repulsive interactions between monomers that hinder fibril assembly. The effects of charging the α-amino group are much smaller than with His18 (Figure 3A,B), consistent with the location of the latter site in the β-sheet core of the amylin fibril structure model.[8,50]

Influence of Salt on the pK_a of His18 in Amylin Fibrils. The lowered pK_a value of His18 in the fibrils and the inhibition of fibril formation when the histidine becomes charged at low pH suggest that protonation of this site leads to electrostatic repulsion between positive charges in adjacent monomers stacked along the fibril axis. To further test this mechanism, we looked at the effects of increasing NaCl concentration on the pK_a of His18, because salt should screen the positive charge at this site and thus alleviate the inhibition of fibril formation. For these studies, we used NAc-amylin because His18 is the only titratable site in this peptide. The effects of salt on the pK_a value of His18 are summarized in Figure 5. Data are shown from ThT (gray bars) and Nile Red (white bars) experiments at 0, 150, and 300 mM NaCl, while turbidimetry (black bars) was only used to study fibril formation in the absence of salt. In the absence of salt, the ThT data may contain contributions from both the peptide and the dye. As described previously, however, the effects of the dye ThT are suppressed in the presence of 150 or 300 mM NaCl. The Nile Red and turbidimetry experiments measure contributions exclusively from His18 in the peptide.

In the absence of salt, the pK_a value of His18 is lowered by ~1.5 pH units relative to that of a histidine in a random coil (Figure 5). With an increasing NaCl concentration, the pK_a value of His18 approaches the limiting value of a histidine in a random coil conformation (pK_a = 6.5) according to both the ThT and Nile Red data. At a physiological ionic strength of 150 mM NaCl, the pK_a of His18 is still lowered by approximately 0.5−1.0 pH unit compared to the random coil value. The pK_a shift generally appears to be larger for the lag times than for the elongation rates (Figure 5). A possible explanation is that electrostatic repulsion is more significant for the formation of the critical nuclei but, once these are formed, becomes less of an impeding factor for the addition of monomers to the growing fibrils.

The Presence of a Charged Side Chain at Position 18 Affects Fibril Morphology and Amylin Cytotoxicity. Figure 6 compares EM images of wt amylin at neutral (Figure 6A) and acidic pH (Figure 6B). As previously described,[34,48]

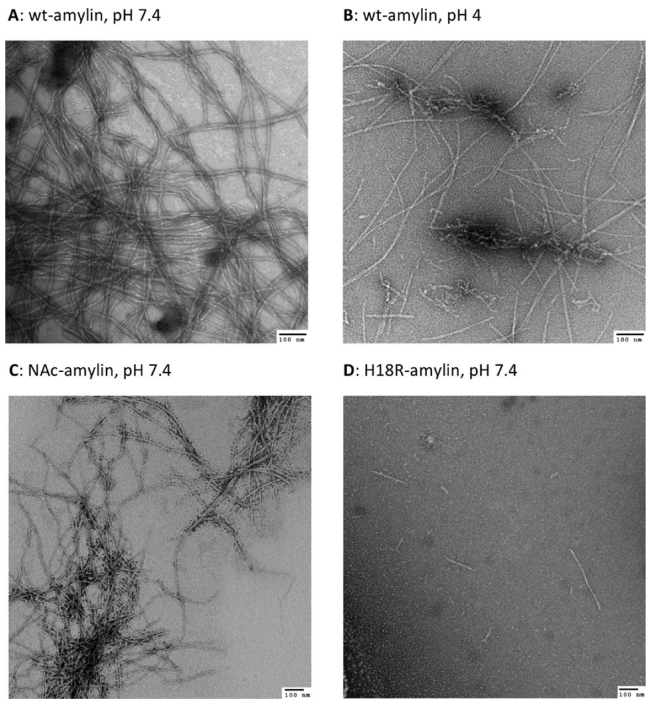

Figure 6. Electron micrographs of amylin fibrils: (A) wt amylin at pH 7.4, (B) wt amylin at pH 4.0, (C) NAc-amylin at pH 7.4, and (D) H18R amylin at pH 7.4.

dx.doi.org/10.1021/bi401164k | *Biochemistry* 2014, 53, 300−310

there are fewer fibrils formed at acidic pH when His18 is charged, and the fibrils have a different morphology by EM. Compared to the fibrils formed at acidic pH, the fibrils at neutral pH are longer and thicker, have a more pronounced coil-like twist, and more often associate into bundles. The same trends are seen when NAc-amylin (Figure 6C), which has an uncharged His18 at neutral pH, is compared with H18R amylin (Figure 6D), which replaces the histidine with a permanently charged arginine. The smaller amounts of fibrils formed for H18R amylin compared to NAc-amylin by EM are consistent with steady-state fluorescence plateaus, which are ∼10-fold smaller with ThT and 3-fold smaller with Nile Red for H18R amylin than for NAc-amylin at pH 7.4 (Figure S11 of the Supporting Information). Taken together, these observations suggest that the presence of a positively charged side chain at position 18, which is involved in the hydrogen-bonded β-sheet of the structural model for the fibrils,[8,50] inhibits fibrillization and hinders the lateral association of fibrils into bundles.

The presence of a charged side chain at position 18 also affects amylin cytotoxicity toward a MIN6 mouse insuloma model of pancreatic β-cells (Figure 7). Similar losses of cell viability were seen when wt amylin and NAc-amylin were added to MIN6 cell cultures. Both these peptides have an uncharged His18 under the physiological pH conditions of the experiments (pH 7.4). With H18R amylin, in which a permanently charged arginine is substituted for the histidine, cell viability was comparable to that seen in the control experiments without amylin. Decreased cytotoxicity with the H18R substitution was previously reported in the context of a 1−19 fragment of amylin.[53]

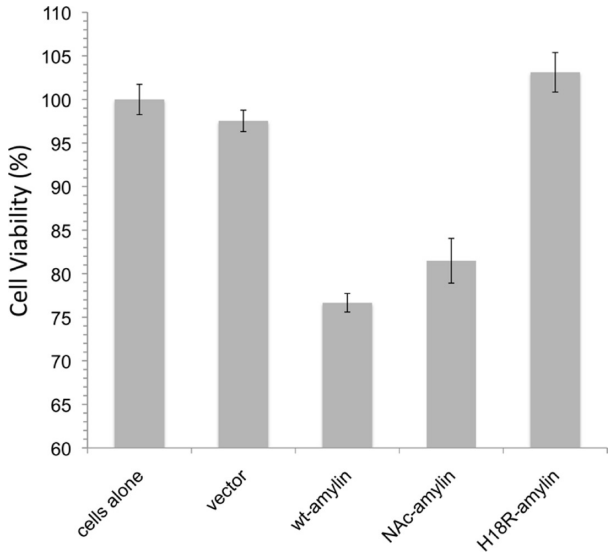

Figure 7. Cytotoxicity experiments using cultures of a MIN6 mouse insuloma model of β-pancreatic cells. Data are expressed as means ± SEM from triplicate measurements. Peptides were prepared as stock solutions in DMSO and were freshly added to the cells to give a final peptide concentration of 80 μM as measured with a micro-BCA assay, and a final DMSO concentration of 1% (v/v). The vector control contained 1% DMSO only, which was present in all experiments except the first.

DISCUSSION

The motivation for these studies was to examine the roles of charge−charge interactions in amyloid fibril formation. Replacements of single charged residues can have large effects on fibrillization kinetics as shown with amyloid-β,[10] α-synuclein,[54,55] and amylin.[15] These observations suggest that electrostatic interactions play important roles in fibril assembly. Amylin is an ideal system for quantifying the contributions of ionizable sites to fibrillization. The use of single-site peptide variants, housing only one of the two ionizable sites in amylin, made it possible to determine contributions from individual charged residues to fibril formation.

The α-amino group in the fibrillar state of amylin has a pK_a value of ∼8.0, close to the random coil limit. Charging of the α-amino group leads to a relatively modest inhibition of fibrillization (Figure S9 of the Supporting Information). The small effects of the α-amino group are consistent with its location in a disordered part of the amylin fibril structure model.[8,50]

Ionization of His18, which is part of the intermolecular β-sheet of amylin protofibrils in the ssNMR structure model,[8,50] causes a stronger inhibition of fibrillization as manifested by larger reductions in elongation rates and increases in lag times (Figure S9 of the Supporting Information). The apparent pK_a of His18 in the fibrils, measured from the pH dependence of the lag times or fibrillization rates (Figures 4 and 5), is 1.5 pH units smaller than that for a histidine in a random coil. Because amyloid fibril assemblies likely involve coupling between charges replicated along the length of the fibril,[56] the pK_a values reported for fibrils in this work are best considered as apparent, averaged ionization constants, rather than distinct ionization constants for a given site. Nevertheless, the shift of the apparent pK_a of His18 in the fibrils to a more acidic value than in random coil models indicates that the histidine requires a higher proton concentration to become charged in the fibrils and that addition of a charge to this site is energetically unfavorable. There are two mechanisms that could account for the lowered pK_a value of His18 in the fibrils. The histidine could be immersed in a relatively hydrophobic environment in the fibrils. The lower dielectric constant of this environment would resist addition of a charge. In the ssNMR structural model of amylin protofibrils,[8] His18 is in a relatively solvent-exposed location on the surfaces of two stacks of intermolecular β-sheets related by C_2 symmetry. Alternatively, the proximity of charged histidines on adjacent monomers along the length of the fibril would lead to electrostatic repulsion, particularly as there are no negatively charged groups in amylin to complement the positive charges. With an increasing NaCl concentration, the apparent pK_a of His18 shifts toward the random coil limit (Figure 5). The screening by salt suggests that electrostatic repulsion is a more important contribution to the inhibition of fibrillization than the burial of His18 in a hydrophobic environment. In this regard, it is interesting to note that a recent molecular dynamics investigation of the amylin protofibril structure suggests that electrostatic repulsion between His18 residues stacked along the fibril axis is a principal factor in the inhibition of fibrillization at acidic pH.[57] In this sense, His18 appears to act as an electrostatic switch that facilitates amylin fibril formation in its neutral state but opposes aggregation in its charged state.

The charged state of His18 affects the morphology of amylin fibrils as determined by EM. We have confirmed the observation that at physiological pH where His18 is uncharged, wt amylin forms a greater number of fibrils.[34,48] The fibrils at neutral pH are longer, have a more twisted morphology, and are more likely to be laterally associated into bundles (Figure

6A) than the fibrils formed at acidic pH where His18 is charged (Figure 6B). The morphological features of wt amylin at acidic pH are reproduced at physiological pH when a permanently charged arginine replaces the histidine in the H18R amylin mutant (Figure 6D). His18 is located on the surface of the amylin protofibril structural model determined by ssNMR.[8,50] Electrostatic repulsion between adjacent monomers stacked along the fibril axis may account for the observations that fewer fibrils are formed by EM and that when these occur they are frequently shorter when position 18 is occupied by a charged residue (Figure 6B,D). Moreover, the presence of a charged residue at position 18 would give the surfaces of the protofibrils a more positive character, which may account for the weakened tendency of H18R amylin and wt amylin at acidic pH to associate laterally into higher-order bundles (Figure 6B,D).

The presence of a charged arginine at position 18 in H18R amylin lowers the cytotoxicity to MIN6 β-cells compared to that of wt amylin or NAc-amylin (Figure 7), each of which has an uncharged histidine at a physiological pH of 7.4. It is tempting to conclude that the decreased cytotoxicity of H18R amylin is related to the different morphology of the fibrils observed by EM (Figure 6); however, other mechanisms are possible. The decreased cytotoxicity of H18R amylin could simply be a consequence of the weaker propensity of this variant to aggregate, as exemplified by its smaller fluorescence plateaus (Figure S11 of the Supporting Information) and the decreased amounts of fibrils formed by EM (Figure 6D). Another possible mechanism, based on a study of a 1−19 fragment of the 37-residue amylin peptide, is that the ability of amylin to disrupt β-cell membranes is impaired by the H18R mutation.[53]

In addition to charges on the peptide, we have shown that the fibrillization of amylin can be inhibited by the dye ThT, which is often used to detect fibrils. In its doubly charged state below pH 5, the ThT dye markedly increases the lag times for fibrillization in the absence of salt (Figure 4). These observations suggest caution in the use of ThT for monitoring the pH dependence of fibrillization. Not only do the different charged forms of the dye affect the kinetics of fibril formation but the apparent pK_a near 4.0 that occurs due to ionization of ThT is close to the values typical of histidines and acidic groups (Asp and Glu) in proteins. The most effective way to characterize the pH dependence of amyloid fibril formation is to use multiple methods, when possible. Because amylin contains no negatively charged residues, inhibition is likely to occur through electrostatic repulsion between the positive charges on the ThT dye and positively charged groups on the peptide. The inhibitory effects of ThT are strongly affected by ionic strength and become negligible at physiological or higher salt concentrations. By contrast, the perturbed pK_a values of His18 and the inhibition of fibrillization by the charged form of the histidine persist, albeit to a lesser degree in the presence of salt. The more effective screening of charges on ThT by salt may be due to a higher solvent accessibility for the dye compared to His18.

Taken together, our work suggests that electrostatic repulsion between like charges replicated along the length of the fibril is a major force opposing assembly of polypeptide monomers into amyloid fibrils. We are currently exploiting this principle to design peptide variants that incorporate strings of like-charged residues in the amylin amino acid sequence, to inhibit amylin fibrillogenesis and cytotoxicity.

■ ASSOCIATED CONTENT

Supporting Information

Eleven figures showing the effects of pH and NaCl concentration on fibril formation by the SNNFGAILSS peptide, wt amylin, NAc-amylin, and H18R amylin as monitored by ThT, Nile Red, and turbidimetry, spectroscopic properties of the Nile Red dye, and comparisons of NAc-amylin and H18R amylin fibrillization reaction profiles. This material is available free of charge via the Internet at http://pubs.acs.org.

■ AUTHOR INFORMATION

Corresponding Author

*Department of Molecular and Cell Biology, University of Connecticut, 91 N. Eagleville Rd., Storrs, CT 06269-3125. E-mail: andrei@uconn.edu. Telephone: (860) 486-4414. Fax: (860) 486-4331.

Present Address

†S.J.: Department of Life Sciences, National Institute of Technology, Rourkela 769008, Orissa, India.

Funding

This work was supported by an American Diabetes Association Basic Science Award to A.T.A., a National Science Foundation Graduate Research Fellowship to S.R.S., and a UConn Summer Undergraduate Research Fellowship to J.M.S.

Notes

The authors declare no competing financial interest.

■ ACKNOWLEDGMENTS

We thank Prof. C. Vijay Kumar for useful discussions about fluorescence and Prof. Craig E. Nelson for advice on cytotoxicity measurements.

■ ABBREVIATIONS

DMSO, dimethyl sulfoxide; EM, electron microscopy; NMR, nuclear magnetic resonance; SEM, standard error of the mean; ssNMR, solid-state NMR; ThT, thioflavin T.

■ REFERENCES

(1) *IDF Diabetes Atlas*, 5th ed. (2011) International Diabetes Federation, Brussels.

(2) Hayden, M. R., Tyagi, S. C., Kerklo, M. M., and Nicolls, M. R. (2005) Type 2 diabetes mellitus as a conformational disease. *JOP: Journal of the Pancreas 6*, 287−302.

(3) Cooper, G. J. (1994) Amylin compared with calcitonin gene-related peptide: Structure, biology, and relevance to metabolic disease. *Endocr. Rev. 15*, 163−201.

(4) Westermark, P., Andersson, A., and Westermark, G. T. (2011) Islet amyloid polypeptide, islet amyloid, and diabetes mellitus. *Physiol. Rev. 91*, 795−826.

(5) Cao, P., Abedini, A., and Raleigh, D. P. (2013) Aggregation of islet amyloid polypeptide: From physical chemistry to cell biology. *Curr. Opin. Struct. Biol. 23*, 82−89.

(6) Patil, S. M., Xu, S., Sheftic, S. R., and Alexandrescu, A. T. (2009) Dynamic α-helix structure of micelle-bound human amylin. *J. Biol. Chem. 284*, 11982−11991.

(7) Alexandrescu, A. T., and Croke, R. L. (2008) NMR of Amyloidogenic Proteins. In *Protein Misfolding* (O'Doherty, C. B., and Byrne, A. C., Eds.) Nova Science Publishers, Hauppauge, NY.

(8) Luca, S., Yau, W. M., Leapman, R., and Tycko, R. (2007) Peptide conformation and supramolecular organization in amylin fibrils: Constraints from solid-state NMR. *Biochemistry 46*, 13505−13522.

(9) Calamai, M., Kumita, J. R., Mifsud, J., Parrini, C., Ramazzotti, M., Ramponi, G., Taddei, N., Chiti, F., and Dobson, C. M. (2006) Nature

and significance of the interactions between amyloid fibrils and biological polyelectrolytes. *Biochemistry 45*, 12806−12815.
(10) Sheftic, S. R., Croke, R. L., LaRochelle, J. R., and Alexandrescu, A. T. (2009) Electrostatic contributions to the stabilities of native proteins and amyloid complexes. *Methods Enzymol. 466*, 233−258.
(11) Alexandrescu, A. T. (2005) Amyloid accomplices and enforcers. *Protein Sci. 14*, 1−12.
(12) Jha, S., Patil, S. M., Gibson, J., Nelson, C. E., Alder, N. N., and Alexandrescu, A. T. (2011) Mechanism of amylin fibrillization enhancement by heparin. *J. Biol. Chem. 286*, 22894−22904.
(13) Westermark, G. T., Westermark, P., Berne, C., and Korsgren, O. (2008) Widespread amyloid deposition in transplanted human pancreatic islets. *N. Engl. J. Med. 359*, 977−979.
(14) Potter, K. J., Abedini, A., Marek, P., Klimek, A. M., Butterworth, S., Driscoll, M., Baker, R., Nilsson, M. R., Warnock, G. L., Oberholzer, J., Bertera, S., Trucco, M., Korbutt, G. S., Fraser, P. E., Raleigh, D. P., and Verchere, C. B. (2010) Islet amyloid deposition limits the viability of human islet grafts but not porcine islet grafts. *Proc. Natl. Acad. Sci. U.S.A. 107*, 4305−4310.
(15) Cao, P., Tu, L. H., Abedini, A., Levsh, O., Akter, R., Patsalo, V., Schmidt, A. M., and Raleigh, D. P. (2012) Sensitivity of amyloid formation by human islet amyloid polypeptide to mutations at residue 20. *J. Mol. Biol. 421*, 282−295.
(16) Ma, Z., Westermark, G. T., Sakagashira, S., Sanke, T., Gustavsson, A., Sakamoto, H., Engstrom, U., Nanjo, K., and Westermark, P. (2001) Enhanced in vitro production of amyloid-like fibrils from mutant (S20G) islet amyloid polypeptide. *Amyloid 8*, 242−249.
(17) Sakagashira, S., Sanke, T., Hanabusa, T., Shimomura, H., Ohagi, S., Kumagaye, K. Y., Nakajima, K., and Nanjo, K. (1996) Missense mutation of amylin gene (S20G) in Japanese NIDDM patients. *Diabetes 45*, 1279−1281.
(18) Xu, W., Jiang, P., and Mu, Y. (2009) Conformation preorganization: Effects of S20G mutation on the structure of human islet amyloid polypeptide segment. *J. Phys. Chem. B 113*, 7308−7314.
(19) Rhodes, C. J. (2005) Type 2 diabetes: A matter of β-cell life and death? *Science 307*, 380−384.
(20) Janson, J., Ashley, R. H., Harrison, D., McIntyre, S., and Butler, P. C. (1999) The mechanism of islet amyloid polypeptide toxicity is membrane disruption by intermediate-sized toxic amyloid particles. *Diabetes 48*, 491−498.
(21) Lorenzo, A., Razzaboni, B., Weir, G. C., and Yankner, B. A. (1994) Pancreatic islet cell toxicity of amylin associated with type-2 diabetes mellitus. *Nature 368*, 756−760.
(22) Anguiano, M., Nowak, R. J., and Lansbury, P. T., Jr. (2002) Protofibrillar islet amyloid polypeptide permeabilizes synthetic vesicles by a pore-like mechanism that may be relevant to type II diabetes. *Biochemistry 41*, 11338−11343.
(23) Engel, M. F. (2009) Membrane permeabilization by islet amyloid polypeptide. *Chem. Phys. Lipids 160*, 1−10.
(24) Haataja, L., Gurlo, T., Huang, C. J., and Butler, P. C. (2008) Islet amyloid in type 2 diabetes, and the toxic oligomer hypothesis. *Endocr. Rev. 29*, 303−316.
(25) Meng, F., Marek, P., Potter, K. J., Verchere, C. B., and Raleigh, D. P. (2008) Rifampicin does not prevent amyloid fibril formation by human islet amyloid polypeptide but does inhibit fibril thioflavin-T interactions: Implications for mechanistic studies of β-cell death. *Biochemistry 47*, 6016−6024.
(26) Engel, M. F., Khemtemourian, L., Kleijer, C. C., Meeldijk, H. J., Jacobs, J., Verkleij, A. J., de Kruijff, B., Killian, J. A., and Hoppener, J. W. (2008) Membrane damage by human islet amyloid polypeptide through fibril growth at the membrane. *Proc. Natl. Acad. Sci. U.S.A. 105*, 6033−6038.
(27) Carulla, N., Caddy, G. L., Hall, D. R., Zurdo, J., Gairi, M., Feliz, M., Giralt, E., Robinson, C. V., and Dobson, C. M. (2005) Molecular recycling within amyloid fibrils. *Nature 436*, 554−558.
(28) Janson, J., Soeller, W. C., Roche, P. C., Nelson, R. T., Torchia, A. J., Kreutter, D. K., and Butler, P. C. (1996) Spontaneous diabetes mellitus in transgenic mice expressing human islet amyloid polypeptide. *Proc. Natl. Acad. Sci. U.S.A. 93*, 7283−7288.
(29) Matveyenko, A. V., and Butler, P. C. (2006) Islet amyloid polypeptide (IAPP) transgenic rodents as models for type 2 diabetes. *ILAR J. 47*, 225−233.
(30) Jha, S., Sellin, D., Seidel, R., and Winter, R. (2009) Amyloidogenic propensities and conformational properties of ProIAPP and IAPP in the presence of lipid bilayer membranes. *J. Mol. Biol. 389*, 907−920.
(31) Yonemoto, I. T., Kroon, G. J., Dyson, H. J., Balch, W. E., and Kelly, J. W. (2008) Amylin proprotein processing generates progressively more amyloidogenic peptides that initially sample the helical state. *Biochemistry 47*, 9900−9910.
(32) Jaikaran, E. T., Nilsson, M. R., and Clark, A. (2004) Pancreatic β-cell granule peptides form heteromolecular complexes which inhibit islet amyloid polypeptide fibril formation. *Biochem. J. 377*, 709−716.
(33) Knight, J. D., Williamson, J. A., and Miranker, A. D. (2008) Interaction of membrane-bound islet amyloid polypeptide with soluble and crystalline insulin. *Protein Sci. 17*, 1850−1856.
(34) Abedini, A., and Raleigh, D. P. (2005) The role of His-18 in amyloid formation by human islet amyloid polypeptide. *Biochemistry 44*, 16284−16291.
(35) Mishra, R., Sjolander, D., and Hammarstrom, P. (2011) Spectroscopic characterization of diverse amyloid fibrils in vitro by the fluorescent dye Nile red. *Mol. BioSyst. 7*, 1232−1240.
(36) Alexandrescu, A. T., and Rathgeb-Szabo, K. (1999) An NMR investigation of solution aggregation reactions preceding the misassembly of acid-denatured cold shock protein A into fibrils. *J. Mol. Biol. 291*, 1191−1206.
(37) Andreu, J. M., and Timasheff, S. N. (1986) The measurement of cooperative protein self-assembly by turbidity and other techniques. *Methods Enzymol. 130*, 47−59.
(38) Miyazaki, J., Araki, K., Yamato, E., Ikegami, H., Asano, T., Shibasaki, Y., Oka, Y., and Yamamura, K. (1990) Establishment of a pancreatic β cell line that retains glucose-inducible insulin secretion: Special reference to expression of glucose transporter isoforms. *Endocrinology 127*, 126−132.
(39) Hortschansky, P., Schroeckh, V., Christopeit, T., Zandomeneghi, G., and Fandrich, M. (2005) The aggregation kinetics of Alzheimer's β-amyloid peptide is controlled by stochastic nucleation. *Protein Sci. 14*, 1753−1759.
(40) Volles, M. J., and Lansbury, P. T., Jr. (2007) Relationships between the sequence of α-synuclein and its membrane affinity, fibrillization propensity, and yeast toxicity. *J. Mol. Biol. 366*, 1510−1522.
(41) Shoemaker, D. P., Garland, C. W., Steinfeld, J. I., and Nibler, J. W. (1981) *Experiments in Physical Chemistry*, McGraw-Hill, New York.
(42) Thurlkill, R. L., Grimsley, G. R., Scholtz, J. M., and Pace, C. N. (2006) pK values of the ionizable groups of proteins. *Protein Sci. 15*, 1214−1218.
(43) Klunk, W. E., Wang, Y., Huang, G. F., Debnath, M. L., Holt, D. P., and Mathis, C. A. (2001) Uncharged thioflavin-T derivatives bind to amyloid-β protein with high affinity and readily enter the brain. *Life Sci. 69*, 1471−1484.
(44) Naik, L. R., Naik, A. B., and Pal, H. (2009) Steady-state and time-reolved emission studies of thioflavin-T. *J. Photochem. Photobiol., A 204*, 161−167.
(45) Ishihara, H., Asano, T., Tsukuda, K., Katagiri, H., Inukai, K., Anai, M., Kikuchi, M., Yazaki, Y., Miyazaki, J. I., and Oka, Y. (1993) Pancreatic β cell line MIN6 exhibits characteristics of glucose metabolism and glucose-stimulated insulin secretion similar to those of normal islets. *Diabetologia 36*, 1139−1145.
(46) Moriarty, D. F., and Raleigh, D. P. (1999) Effects of sequential proline substitutions on amyloid formation by human amylin20−29. *Biochemistry 38*, 1811−1818.
(47) Sulatskaya, A. I., Kuznetsova, I. M., and Turoverov, K. K. (2012) Interaction of thioflavin T with amyloid fibrils: Fluorescence quantum yield of bound dye. *J. Phys. Chem. B 116*, 2538−2544.

(48) Patil, S. M., Mehta, A., Jha, S., and Alexandrescu, A. T. (2011) Heterogeneous amylin fibril growth mechanisms imaged by total internal reflection fluorescence microscopy. *Biochemistry 50*, 2808−2819.
(49) Khemtemourian, L., Domenech, E., Doux, J. P., Koorengevel, M. C., and Killian, J. A. (2011) Low pH acts as inhibitor of membrane damage induced by human islet amyloid polypeptide. *J. Am. Chem. Soc. 133*, 15598−15604.
(50) Alexandrescu, A. T. (2013) Amide proton solvent protection in amylin fibrils probed by quenched hydrogen exchange NMR. *PLoS One 8*, No. e56467.
(51) Mishra, R., Sorgjerd, K., Nystrom, S., Nordigarden, A., Yu, Y. C., and Hammarstrom, P. (2007) Lysozyme amyloidogenesis is accelerated by specific nicking and fragmentation but decelerated by intact protein binding and conversion. *J. Mol. Biol. 366*, 1029−1044.
(52) Wolfe, L. S., Calabrese, M. F., Nath, A., Blaho, D. V., Miranker, A. D., and Xiong, Y. (2010) Protein-induced photophysical changes to the amyloid indicator dye thioflavin T. *Proc. Natl. Acad. Sci. U.S.A. 107*, 16863−16868.
(53) Brender, J. R., Hartman, K., Reid, K. R., Kennedy, R. T., and Ramamoorthy, A. (2008) A single mutation in the nonamyloidogenic region of islet amyloid polypeptide greatly reduces toxicity. *Biochemistry 47*, 12680−12688.
(54) Greenbaum, E. A., Graves, C. L., Mishizen-Eberz, A. J., Lupoli, M. A., Lynch, D. R., Englander, S. W., Axelsen, P. H., and Giasson, B. I. (2005) The E46K mutation in α-synuclein increases amyloid fibril formation. *J. Biol. Chem. 280*, 7800−7807.
(55) Paleologou, K. E., Schmid, A. W., Rospigliosi, C. C., Kim, H. Y., Lamberto, G. R., Fredenburg, R. A., Lansbury, P. T., Jr., Fernandez, C. O., Eliezer, D., Zweckstetter, M., and Lashuel, H. A. (2008) Phosphorylation at Ser-129 but not the phosphomimics S129E/D inhibits the fibrillation of α-synuclein. *J. Biol. Chem. 283*, 16895−16905.
(56) Cao, P., Marek, P., Noor, H., Patsalo, V., Tu, L. H., Wang, H., Abedini, A., and Raleigh, D. P. (2013) Islet amyloid: From fundamental biophysics to mechanisms of cytotoxicity. *FEBS Lett. 587*, 1106−1118.
(57) Li, Y., Xu, W., Mu, Y., and Zhang, J. Z. (2013) Acidic pH retards the fibrillization of human islet amyloid polypeptide due to electrostatic repulsion of histidines. *J. Chem. Phys. 139*, 055102.